

Neural network based approach for rapid prediction of deflections in RC beams considering cracking

K. A. Patel^{1a}, Sandeep Chaudhary^{*2} and A. K. Nagpal^{1b}

¹Department of Civil Engineering, Indian Institute of Technology Delhi, 110016, New Delhi, India

²Department of Civil Engineering, Malaviya National Institute of Technology Jaipur, 302017, Jaipur, India

(Received July 26, 2016, Revised December 3, 2016, Accepted December 28, 2016)

Abstract. Maximum deflection in a beam is a serviceability design criterion and occurs generally at or close to the mid-span. This paper presents a methodology using neural networks for rapid prediction of mid-span deflections in reinforced concrete beams subjected to service load. The closed form expressions are further obtained from the trained neural networks. The closed form expressions take into account cracking in concrete at in-span and at near the interior supports and tension stiffening effect. The expressions predict the inelastic deflections (incorporating the concrete cracking) from the elastic moments and the elastic deflections (neglecting the concrete cracking). Five separate neural networks are trained since these have been postulated to represent all beams having any number of spans. The training, validating, and testing data sets for the neural networks are generated using an analytical-numerical procedure of analysis. The proposed expressions have been verified by comparison with the experimental results reported elsewhere and also by comparison with the finite element method (FEM). The proposed expressions, at minimal input data and minimal computation effort, yield results that are close to FEM results. The expressions can be used in every day design since the errors are found to be small.

Keywords: closed form expression; cracking; deflection; neural network; reinforced concrete; service load

1. Introduction

The reinforced concrete (RC) continuous beams are subjected the hogging moment near the ends and sagging moments in the middle portion of the members (Fig. 1). When these moments are higher than the cracking moments, cracking takes place near the interior supports and in the middle portion of an intermediate span of a RC continuous beam as shown in Fig. 1. This cracking may result in considerable change in deflections of the continuous beams due to much reduced stiffness of members. The appropriate prediction of deflections after moment redistribution owing to the concrete cracking is important from serviceability considerations.

Different procedures are available in the literature for taking into account the concrete cracking and other non-linear effects in the analysis of RC beams. The procedures may be categorised in two types: Type 1 and Type 2. In Type 1 procedures (Wang and Hsu 2001, Yang and Chen 2005, Stramandinoli and Rovere 2008, 2012, Mohr *et al.* 2010, Casanova *et al.* 2012, Dai *et al.* 2012), members are discretized into a number of elements along the length and across the cross-section. In Type 2 procedures (Chan *et al.*

2000a, b, Tanrikulu *et al.* 2000, Dundar and Kara 2007, Kara and Dundar 2009, 2010), the average moment of inertia along the member length is represented by the effective moment of inertia of members and the transformed section properties are considered. Both these types of procedures are based either on an incremental or iterative approach, and therefore, require a computational effort, which is many times more than the required for the elastic analysis (neglecting cracking).

In codes of practice (ACI 318 2008, CSA A23.3 2004), for simply supported beams, a simplified expression based on effective moment of inertia is available for estimation of deflections. However, this expression is not appropriate since under-estimation of deflections for lightly reinforced members has been reported (Scanlon *et al.* 2001, Bischoff 2005, Kalkan 2010, Patel *et al.* 2015, 2016a). Some researchers (Scanlon *et al.* 2001, Bischoff 2005) have modified the expression for improvement in prediction of results, however, an expression proposed by Bischoff (2005) is found most accurate (Kalkan 2010). Furthermore, this expression is also used to evaluate a weighted average effective moment of inertia for continuous beams in accordance with ACI 435 (2000) procedure. However, the accuracy in deflections resulting from the procedure needs to be investigated. Also no simplified expressions are available for rapid prediction of deflections in such beams. The appropriate prediction of deflections in continuous beams for entire practical range of reinforcements is therefore desirable. The use of closed form expressions obtained from the trained neural networks may be made in such cases to rapidly estimate the quantities of design interest for use in everyday design.

*Corresponding author, Ph.D.

E-mail: schaudhary.ce@mnit.ac.in

^aPh.D.

E-mail: iitd.kashyap@gmail.com

^bPh.D.

E-mail: aknagpal@civil.iitd.ac.in

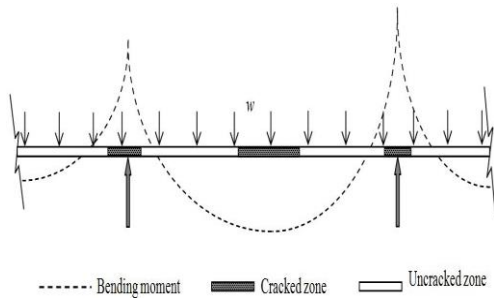


Fig. 1 A typical intermediate span of a RC beam with loads, bending moment, and possible cracked-uncracked zones

Extensive literature is available on the use of neural networks for prediction of behaviour of structures without any rigorous analysis and experiments (Pala 2006, Chaudhary *et al.* 2007, 2014, Pendharkar *et al.* 2007, 2010, 2011, 2015, 2016a, b, Shahin and Elchalakani 2008, Caglar *et al.* 2009, Kim *et al.* 2009, Dias and Silvestre 2011, Saechai *et al.* 2011, 2012, Khan 2012, Tadesse *et al.* 2012, Gupta *et al.* 2013, 2015, Mohammadhassani *et al.* 2013a, b, Tohidi and Sharifi 2015). Closed form expressions have been proposed by many researchers using the weight matrices, biases and activated functions of the trained networks. Such expressions are useful to estimate the quantities of design interest for use in everyday design with acceptable accuracy. Researchers have proposed expressions for distortional buckling stress in steel members (Pala 2006, Dias and Silvestre 2011), inelastic distortional buckling capacity in steel beams (Tohidi and Sharifi 2015), ultimate pure bending of fabricated and cold-formed steel circular tubes (Shahin and Elchalakani 2008), base shear of steel frame structures (Caglar *et al.* 2009) and for deflections in composite bridges (Tadesse *et al.* 2012, Gupta *et al.* 2013, 2015). This demonstrates the strength of neural networks in predicting the solutions of different structural engineering problems.

In this paper, a methodology using neural networks has been proposed for rapid prediction of inelastic deflections in RC continuous beams subjected to service load. The closed form expressions obtained from the trained neural networks take into account concrete cracking, tension stiffening effect and entire practical range of reinforcements. The expressions predict the inelastic mid-span deflections, D^{in} (considering the concrete cracking) from the elastic moments, M^{el} and the elastic mid-span deflections, D^{el} (neglecting the concrete cracking). M^{el} and D^{el} , in turn, can be obtained from any of the readily available software. The expressions enable rapid estimation of inelastic deflections and require a computational effort that is a fraction of that required for Type 1 and Type 2 procedures available in the literature. The proposed expressions are verified by comparison with the experimental results reported elsewhere and also by comparison with finite element method (FEM) for a number of example beams. The errors are shown to be small for practical purposes. The methodology can be extended for large RC building frames where a very significant saving in computational effort would result.

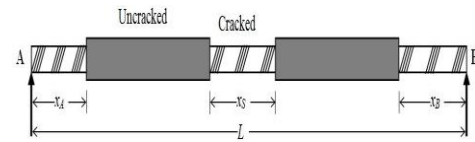


Fig. 2 A cracked span length beam element

2. Analytical-numerical procedure for analysis of RC beams

For generalized and efficient neural networks, a huge number of training, validating and testing data sets are required for which a highly computationally efficient method is desirable. Recently, Patel *et al.* (2014) have developed an analytical-numerical procedure to take into account concrete cracking within the spans and near the interior supports and reinforcement variation along the span in RC beams. The procedure is analytical at the element level and numerical at the structural level. A cracked span length beam element, consisting of five zones (three cracked zones of lengths x_A , x_B at the ends A and B respectively and x_S , at an in-span position, and two uncracked zones in between the cracked zones), (Fig. 2) has been used in the procedure. The closed form expressions for crack lengths, flexibility matrix coefficients, end displacements and mid-span deflection of the cracked span length beam element are derived and used in the procedure. Tension stiffening effect is also taken into account by evaluating average interpolation coefficients for the cracked zones. The analysis is carried out using an iterative method.

Consider, a typical iterative cycle. A displacement analysis is carried out in the beginning of the cycle for the out-of-balance force vector of the RC beam at the end of the previous cycle. Revised force vector and displacement vector are obtained by adding the force vector and displacement vector obtained from this analysis to the force vector and displacement vector at the end of previous cycle. Crack lengths and interpolation coefficients are then updated according to the revised force vector.

Changes in the cracking state of the sections (cracked or uncracked) and thereby in the end rotations of the beam elements lead to the difference between the displacement vector of these elements obtained from the displacement analysis and that obtained by the principle of virtual work involving integration of curvature diagram of a member. The out-of-balance force vector of beam element corresponding to this error in displacement vector is obtained using the revised flexibility matrix of the beam element.

The out-of-balance force vector of the continuous RC beam (obtained by assembling the out-of-balance force vector of the beam elements) should be within permissible limit (Bathe 2002) for the iterative process to terminate; otherwise a new cycle is started. Required results are obtained after the convergence is achieved.

The procedure has been validated by comparison with the experimental and numerical results available in literature along with FEM results (Patel *et al.* 2014). The results have been found to be in good agreement. The required computational time by the procedure has been

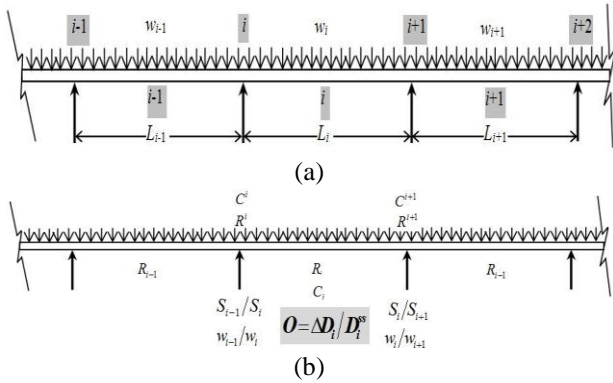


Fig. 3(a) A typical span of a continuous beam and (b) schematic representation of input and output parameters

found to be a small fraction of that required in the FEM.

3. Selection of probable structural parameters

In order to cover a wide range of practical cases, it is required to define important parameters which could be varied to cover all practical situations and can be used as input parameters for generation of data sets.

As stated earlier, cracking in RC beams occurs near the interior supports (where hogging moments occur) and at in-span (where sagging moments occur) when elastic moments are higher than the cracking moments. Owing to cracking, the moment of inertia of sections reduces from that of uncracked section, I^m to that of the cracked section, I^r , thereby reducing the stiffness of the spans. The elastic bending moment, M^{el} gets therefore redistributed and leads to inelastic bending moment, M^{in} . The reduced stiffness and redistributed moments may result in considerable change in the deflections of the continuous beams.

It has been shown in earlier studies for a continuous composite beam (Pendharkar *et al.* 2010, Chaudhary *et al.* 2014), that in order to establish change in the mid-span deflection of any span with sufficient accuracy, cracking at its supports and adjacent supports only needs to be considered. It is therefore assumed that in order to establish change in the mid-span deflection of a span i in RC continuous beam with sufficient accuracy, cracking at the supports (support i and support $i+1$), at the mid of a span i and at the mid of adjacent spans (span $i-1$ and span $i+1$) only needs to be considered (Fig. 3). The subscript, i and superscript, i here and subsequently in other quantities indicate that the quantities are evaluated at a mid of a span i and at a support i respectively. Fig. 3(a) shows an intermediate portion of a continuous beam with internal span i and adjacent spans $i-1$ and $i+1$ of lengths L_i , L_{i-1} and L_{i+1} and with loadings w_i , w_{i-1} and w_{i+1} respectively. The adjacent supports of the internal span i are support i and support $i+1$.

Considering the above discussion, the parameters affecting the mid-span deflection in a typical span i may be listed as (Fig. 3)

1. Inertia ratio at the mid of the span, C_i , where $C = I^r / I^s$

Table 1 Practical range and sampling point of probable structural input parameters

Parameter	Range	Sampling point	
		Numbers	Values
C^i, C_i, C^{i+1}	0.10-2.00	10	0.1, 0.2, 0.3, 0.5, 0.7, 0.9, 1.2, 1.5, 1.8, 2.0
$R_{i-1}, R^i, R_i, R^{i+1}, R_{i+1}$	0.25-4.00	7	0.25, 0.33, 0.5, 1.0, 2.0, 3.0, 4.0
$S_{i-1}/S_i, S_i/S_{i+1}$	0.25-4.00	7	0.25, 0.33, 0.5, 1.0, 2.0, 3.0, 4.0
$w_{i-1}/w_i, w_i/w_{i+1}$	0.25-4.00	7	0.25, 0.33, 0.5, 1.0, 2.0, 3.0, 4.0

(I^r =transformed moment of inertia of RC section about neutral axis neglecting concrete in tension or cracked moment of inertia of RC section about neutral axis, and I^s =gross moment of inertia of RC section about neutral axis).

2. Inertia ratios at the supports, C^i ; and C^{i+1} .
3. Cracking moment ratios at the mid of the spans, R_{i-1} ; R_i ; and R_{i+1} , where $R = M^{cr} / M^{el}$.
4. Cracking moment ratios at the supports, R^i ; and R^{i+1} .
5. Stiffness ratios of adjacent spans, S_{i-1}/S_i ; and S_i/S_{i+1} ($S_i = E_c I^s / L_i$, where E_c = modulus of elasticity of concrete, and L_i =length of i^{th} span).
6. Load ratios of adjacent spans, w_{i-1}/w_i ; and w_i/w_{i+1} .

Inelastic deflection, D_i^{in} may be obtained from the elastic deflection, D_i^{el} and the output parameter. The ratio D_i^{el} / D_i^{in} and $\Delta D_i / D_i^{ss}$ would be the output parameter of the neural networks for simply supported beams and continuous beams with two and larger number of spans respectively, where, and D_i^{ss} =elastic mid-span deflection (neglecting concrete cracking) of an equivalent simply supported beam with the same span length and the loading as that of the span under consideration. These twelve input and one output parameters are schematically shown in Fig. 3(b). The practical ranges for the probable structural parameters are given in Table 1.

4. Data sets generation for neural networks

A large data set is required to be generated for training, validating and testing to achieve better performance of neural network. The performance in terms of generalization and prediction qualities depends significantly on data sets and the domain this data sets covers.

It is expected that effect of cracking on deflections of simply supported beams, two span beams and multi span beams would be different. Presently, a representative beam having five spans is assumed to represent all beams having three and larger number of spans. However, for continuous beams having spans greater than three, nonlinear effects of cracking in external, penultimate and internal spans are different. It may, further, be assumed that the nonlinear effects of cracking at all internal spans are similar in beams having spans greater than three. Accordingly, three separate data sets are generated for external, penultimate and internal spans of continuous beams having spans greater than three.

The external and internal spans of three span beams are

Table 2 Normalization factors for input and output parameters

Network	Parameters												
	Input											Output	
	C^i	C_i	C^{i+1}	R_{i-1}	R^i	R_i	R^{i+1}	R_{i+1}	S_{i-1}/S_i	S_i/S_{i+1}	w_{i-1}/w_i	w_i/w_{i+1}	O
NET-SS	-	2.0	-	-	-	4.0	-	-	-	-	-	-	1.00
NET-TE	-	2.0	2.0	-	-	4.0	4.0	4.0	-	4.0	-	4.0	4.00
NET-ME	2.0	2.0	2.0	4.0	4.0	4.0	4.0	4.0	4.0	4.0	4.0	4.0	4.40
NET-MP	2.0	2.0	2.0	4.0	4.0	4.0	4.0	4.0	4.0	4.0	4.0	4.0	4.20
NET-MI	-	2.0	2.0	-	-	4.0	4.0	4.0	-	4.0	-	4.0	4.00

assumed to be represented by external and penultimate spans of representative five span beam respectively. Further, two data sets are separately generated, each for simply supported and two span continuous beams. Hence, three sets i.e., simply supported beams, two span beams and five span beams are considered to represent beams with any number of spans.

Only two parameters, C_1 and R_1 are considered for simply supported beams since other parameters do not exist. First, consider the left external span ($i=1$) of a two span continuous beams. Since moment at support i is equal to zero and the parameters R_{i-1} , S_{i-1}/S_i , w_{i-1}/w_i indicate a non-existent parameter, only seven input parameters (C_i , C^{i+1} , R_i , R^{i+1} , R_{i+1} , S_i/S_{i+1} , w_i/w_{i+1} , where $i=1$) need to be considered. Similarly, for the right external span of a two span continuous beam, only seven parameters (C^i , C_i , R_{i-1} , R^i , R_i , S_{i-1}/S_i , w_{i-1}/w_i , where $i=2$) need to be considered. Next, for left and right external spans of a beam with three and larger numbers of spans, the seven input parameters as described above for left and right external spans of a two span continuous beams are considered. For penultimate and internal spans, as discussed in Section 3, twelve input parameters (C^i , C_i , C^{i+1} , R_{i-1} , R^i , R_i , R^{i+1} , R_{i+1} , S_{i-1}/S_i , S_i/S_{i+1} , w_{i-1}/w_i , w_i/w_{i+1}) are considered.

The sampling points of each input parameter (Chaudhary *et al.* 2014), considered for data generation, are shown in Table 1. A combination of sampling points of the input parameters and the corresponding resulting value of the output parameter comprises a data set.

As stated earlier, an analytical-numerical procedure (Patel *et al.* 2014) has been used for data generation. The training data sets have been generated for the combinations of the sampling points of input parameters shown in Table 1. The parameters C_{i-1} , C^i , C_{i+1} , S_{i-1}/S_i , w_{i-1}/w_i can be varied independently and assume values indicated in Table 1. However, the parameters R^{i-1} , R_{i-1} , R^i , R_i , R^{i+1} , are interdependent and it is difficult to vary these independently, therefore one parameter is varied independently and the other parameters are allowed to assume values in the practical range 0.25-4.00. The training sets in which the values of the other parameters fall outside the practical range 0.25-4.00 is not considered.

Five neural networks, one for simply supported beams, one for two span beams and three for multi span (having three and larger number of spans, n) beams are trained. The neural network for simply supported beams is designated as NET-SS. The neural network for two span beams is for the

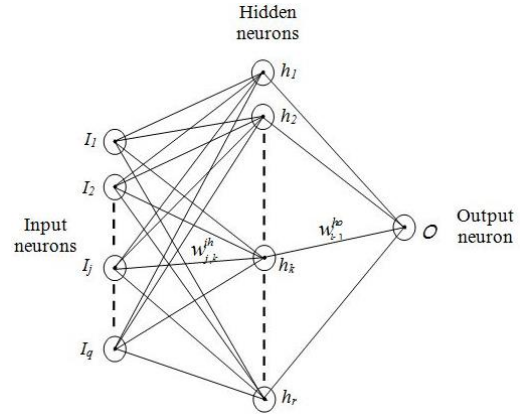


Fig. 4 Configuration of a typical neural network

Table 3 Final architectures and statistical parameters of neural networks

Sets	Parameters	Network (Architecture)				
		NET-SS (2-4-1)	NET-TE (7-10-1)	NET-ME (7-10-1)	NET-MP (12-16-1)	NET-MI (12-16-1)
Training	MSE	0.00060	0.00020	0.00010	0.00010	0.00007
	R^2	0.99399	0.99025	0.99665	0.98918	0.99143
	RMSE	0.02447	0.01414	0.00999	0.00991	0.00836
	MAPE	2.43761	2.44036	4.24471	2.17690	2.31241
	AAD	2.16335	2.31421	3.03770	1.99001	2.16840
	COV	3.46748	3.96892	4.67712	2.91781	3.31823
Validating	MSE	0.00060	0.00021	0.00014	0.00010	0.00007
	R^2	0.99410	0.98993	0.99515	0.98909	0.99153
	RMSE	0.02436	0.01449	0.01177	0.00997	0.00841
	MAPE	2.48549	2.76675	3.79801	2.20533	2.32431
	AAD	2.20885	2.41796	3.29431	1.99915	2.18436
	COV	3.49137	4.11041	5.47448	2.93339	3.33281
Testing	MSE	0.00060	0.00020	0.00010	0.00010	0.00007
	R^2	0.99488	0.99047	0.99625	0.98939	0.99129
	RMSE	0.02424	0.01414	0.01022	0.00999	0.00837
	MAPE	2.32722	2.06726	3.65883	2.16436	2.27304
	AAD	2.06304	2.40611	3.09263	1.99255	2.16495
	COV	3.24511	3.99778	4.80350	2.93449	3.33018

external spans and is designated as NET-TE. The neural networks for external, penultimate and internal spans of multi span beams are designated NET-ME, NET-MP and NET-MI respectively. For data generation of NET-ME, NET-MP and NET-MI, five span continuous beams are considered.

If the parameters R^{i-1} , R_{i-1} , R^i , R_i , R^{i+1} could be varied independently, the upper limit to the number of possible data sets that can be generated for training, validating and testing of the networks NET-TE, NET-ME, NET-MP, and NET-MI would be 1,680,700 ($=10 \times 10 \times 7 \times 7 \times 7 \times 7 \times 7$), 1,680,700 ($=10 \times 10 \times 7 \times 7 \times 7 \times 7 \times 7 \times 7$), 40,353,607,000 ($=10 \times 10 \times 10 \times 7 \times 7$), and 40,353,607,000 ($=10 \times 10 \times 10 \times 7 \times 7$) respectively. As stated above, if one of the parameters R^{i-1} , R_{i-1} , R^i , R_i , R^{i+1} at a

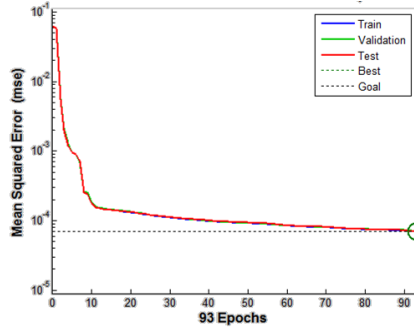


Fig. 5 Variation of the MSE with the epochs (iterations) for network NET-MI

time is varied independently and the other parameters are constrained to assume any values in the practical range 0.25-4.00, the number of data sets gets reduced to 88,710; 6,950; 295,300 and 212,590 for networks NET-TE, NET-ME, NET-MP, and NET-MI respectively. The numbers of data sets for network NET-SS are 70; however, 560 additional data sets have been added for better training. In order to bring all the input and output parameters in the range 0.0 to 1.0, normalization factors are applied to the parameters. The normalization factors for input and output parameters are shown in Table 2. The biases for output parameter of the networks NET-TE, NET-ME, NET-MP, and NET-MI are 1.00, 0.70, 1.40 and 0.95 respectively.

5. Training, architecture and performance of neural networks

The neural networks chosen in the present study are multilayered feed-forward networks with neurons in all the layers fully connected in feed forward manner (Fig. 4). The training is carried out using the MATLAB Neural Network toolbox (MATLAB 2009). Sigmoid function is used as an activation function for the hidden and output neurons and the back propagation learning algorithm is used for training. One hidden layer is chosen and the number of neurons in the layer is decided in the learning process by trial and error.

70% data sets are used for the training and the remaining data sets are divided equally for validating and testing. Similar division has been adopted earlier by other researchers (Gedam *et al.* 2014, Joshi *et al.* 2014). For the training, several trials are carried out with different numbers of neurons in the hidden layer starting with a small number of neurons in the hidden layer and progressively increasing it and checking the mean square errors (MSE) of the training, the validation and the testing. The number of neurons in the hidden layer is decided on the basis of the least mean square errors (MSE) for the training, validation as well testing. Care is taken that the mean square error for test results does not increase with the number of neurons in hidden layer or epochs (overtraining). The final architectures (number of input parameters-number of neurons in the hidden layer-number of output parameters) of all networks along with the statistical parameters i.e., mean square error (MSE), coefficient of correlation (R),

root mean square error (RMSE), mean absolute percentage error (MAPE), average absolute deviation (AAD) and percentage coefficient of variation (COV) of training, validating and testing data sets are given in Table 3. All the parameters indicate a good performance. Typically, for network NET-MI, variation of the MSE with the epochs (iterations) and regressions is shown in Figs. 5 and 6 respectively.

6. Closed form expressions

Simplified closed form expressions can be developed from the trained neural networks, for the rapid prediction of inelastic deflections for ready use by the practicing engineers. The closed form expressions require the values of inputs, weights of the links between the neurons in different layers, and biases of output neurons. Since the sigmoid functions have been used as the activation functions in the hidden and output layer neurons, the output O is given as below (Tadesse *et al.* 2012, Gupta *et al.* 2013, 2015)

$$O = \frac{1}{1 + e^{-\left(bias_o + \sum_{k=1}^r \frac{w_{k,1}^{ho}}{1 + e^{-H_k}} \right)}} \quad (1)$$

$$[H]_{k \times 1} = [w^{ih}]_{k \times j} [I]_{j \times 1} + [bias]_{k \times 1} \quad (2)$$

where, q is the number of input parameters; r is the number of hidden neurons; $bias_k$ is the bias of k^{th} hidden neuron (h_k); $bias_o$ is the bias of output neuron; $w_{j,k}^{ih}$ is the weight of the link between I_j and h_k ; $w_{k,1}^{ho}$ is the weight of the link between h_k and O .

First, consider the simply supported beams. The weights and biases are obtained from the trained neural network NET-SS. As stated earlier, the value of D_i^{el} / D_i^{in} is equal to the output O . The inelastic mid-span deflection, D_i^{in} may be obtained from Eqs. (1)-(2), using weights and biases of NET-SS, as

$$\frac{D_i^{el}}{D_i^{in}} = \frac{1}{1 + e^{-\left(5.60 - \frac{5.87}{1 + e^{-H_1}} + \frac{7.02}{1 + e^{-H_2}} - \frac{11.91}{1 + e^{-H_3}} + \frac{2.60}{1 + e^{-H_4}} \right)}} \quad (3)$$

Where,

$$\begin{bmatrix} H_1 \\ H_2 \\ H_3 \\ H_4 \end{bmatrix} = \begin{bmatrix} -0.71 & -11.56 \\ 4.25 & -17.57 \\ 1.32 & -23.31 \\ 13.67 & -1.60 \end{bmatrix} \begin{bmatrix} C_1 \\ R_1 \end{bmatrix} + \begin{bmatrix} 0.47 \\ 0.99 \\ 3.81 \\ 0.57 \end{bmatrix} \quad (4)$$

Next, consider the continuous beams with two and larger number of spans. As stated earlier, the value of $\Delta D_i / D_i^{ss}$ is equal to the output O . The mid-span deflection of span i from Eq. (1) is then given as

$$D_i^{in} = D_i^{el} + O D_i^{ss} \quad (5)$$

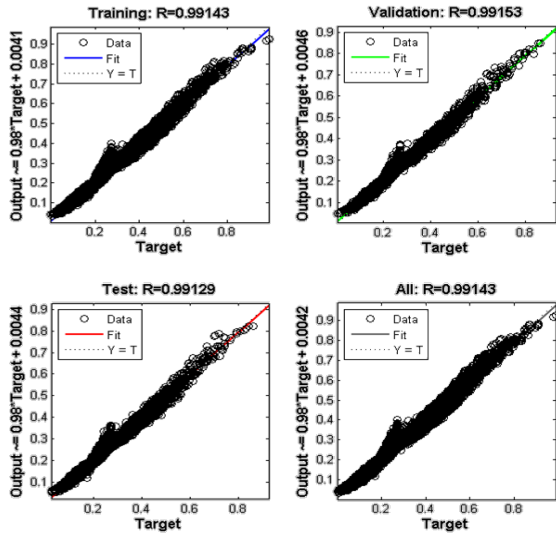


Fig. 5 Regressions of training, validation, testing and all datasets for network NET-MI

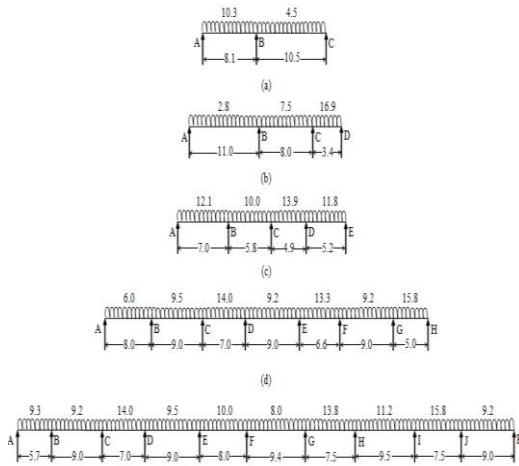


Fig. 6 Example beams: (a) EB1; (b) EB2; (c) EB3; (d) EB4; and (e) EB5 (span lengths in m and loads in kN/m)

The value of O may be obtained from the expressions for external span of two span and external, penultimate and internal spans of multi span continuous beams as given in Appendix A.

7. Verification of the proposed closed form expressions

The proposed closed form expression (Eq. (3)) is verified with experimental results reported by Yu and Winter (1960) for simply supported beams with T cross-section: A-1; B-1; C-1; D-1; E-1; F-1 subjected to uniformly distributed loads, w . The cross-sectional properties (B_f =width of flange, D_f =depth of flange, B_w =width of web, D_w =depth of web, d_t =effective cover at top fibre, d_b =effective cover at bottom fibre, A_{st} =area of reinforcements at top fibre, A_{sb} =area of reinforcements at bottom fibre) and material properties (f_c =cylindrical compressive strength of concrete, E_s =modulus of elasticity

Table 4 Properties of simply supported beams

Properties	Beams					
	A-1	B-1	C-1	D-1	E-1	F-1
B_f (mm)	304.87	304.87	304.87	609.74	304.87	304.87
D_f (mm)	63.52	63.52	63.52	63.52	63.52	50.81
B_w (mm)	152.44	152.44	152.44	152.44	152.44	152.44
D_w (mm)	241.36	241.36	241.36	241.36	241.36	152.44
d_t (mm)	-	39.63	39.63	-	-	-
d_b (mm)	45.98	45.98	45.98	58.94	55.64	45.98
A_{st} (mm ²)	-	200.09	400.19	-	-	-
A_{sb} (mm ²)	400.19	400.19	400.19	774.56	400.19	400.19
f'_c (N/mm ²)	25.37	26.77	24.27	25.37	29.36	29.36
E_c (N/mm ²)	25286	25975	24732	25286	27202	27202
E_s (N/mm ²)	205000	205000	205000	205000	205000	205000
w (N/mm)	6.42	6.44	6.41	11.73	12.29	3.79
f_t (N/mm ²)	2.78	2.66	2.73	2.78	3.06	3.06
L (mm)	6098	6098	6098	6098	4268	6098

Table 5 Comparison of inelastic deflections in the simply supported beams

Mid-span deflections (mm)	Beams					
	A-1	B-1	C-1	D-1	E-1	F-1
D_{CFE}^{in}	29.92	29.69	28.09	32.69	13.79	55.63
D_{EXP}^{in}	34.04	31.50	30.23	32.23	12.96	55.89
D_{FEM}^{in}	33.26	31.31	31.58	32.92	12.87	53.03
D_{ACI}^{in}	28.86	28.88	28.70	31.65	13.61	51.61
D_{BIS}^{in}	28.59	28.60	28.37	31.19	13.74	50.93

of steel reinforcements, f_t =tensile strength of concrete) of the beams are given in Table 4. The mid-span deflections obtained from the proposed closed form expression (D_{CFE}^{in}) and experiments (D_{EXP}^{in}) are reported in Table 5 along with those obtained from FEM (D_{FEM}^{in}), ACI 318 (2008) expression (D_{ACI}^{in}) and Bischoff (2005) expression (D_{BIS}^{in}).

The root mean square percentage errors in D_{CFE}^{in} , D_{FEM}^{in} , D_{ACI}^{in} and D_{BIS}^{in} with respect to D_{EXP}^{in} are 6.74%, 3.08%, 8.30% and 9.17% for all the beams respectively. The deflections obtained from the proposed expression are in good agreement with those obtained from the experiments.

Further, the proposed closed form expressions are also verified for five example beams with a wide variation of input parameters. The example beams (EB1-EB5) are shown schematically in Fig. 7. The cross-sectional properties and f'_c are given in Table 6(a). Additionally, $E_s = 205000$ N/mm², $E_c = 5020\sqrt{f'_c}$ N/mm² and $f_t = 0.623\sqrt{f'_c}$ N/mm² (ACI 318 2008) are taken. As shown in Table 6(b), three segments: left, middle, and right of

Table 6(a) Cross-sectional and material properties

Beams	B_f (mm)	D_f (mm)	B_w (mm)	D_w (mm)	$d_t=d_b$ (mm)	f'_c (N/mm ²)
EB1	400	100	300	300	25	36.60
EB2	-	-	230	450	25	29.65
EB3	350	90	250	350	30	24.91
EB4	-	-	300	300	27	40.38
EB5	300	110	230	200 [*] 270 ^{**}	20	29.65

*For span AB, BC, CD, DE, EF, **For span FG, GH, HI, IJ, JK

Table 6(b) reinforcement detailing data of example beams

Beams	Span	Segment (length)					
		Left (0.25L _i)		Middle (0.50L _i)		Right (0.25L _i)	
		$A_{st}(\rho_{st})$	$A_{sb}(\rho_{sb})$	$A_{st}(\rho_{st})$	$A_{sb}(\rho_{sb})$	$A_{st}(\rho_{st})$	$A_{sb}(\rho_{sb})$
mm ² (%)							
EB1	AB	157 (0.13)	402 (0.34)	157 (0.13)	402 (0.34)	509 (0.42)	226 (0.19)
	BC	509 (0.42)	226 (0.19)	157 (0.13)	402 (0.34)	157 (0.13)	402 (0.34)
EB2	AB	157 (0.15)	509 (0.49)	157 (0.15)	509 (0.49)	760 (0.73)	226 (0.22)
	BC	760 (0.73)	226 (0.22)	157 (0.15)	509 (0.49)	760 (0.73)	226 (0.22)
EB3	BC,CD	226 (0.21)	157 (0.14)	157 (0.14)	226 (0.21)	226 (0.21)	157 (0.14)
	DE	226 (0.21)	157 (0.14)	157 (0.14)	226 (0.21)	157 (0.14)	226 (0.21)
EB4	AB	402 (0.45)	402 (0.45)	402 (0.45)	402 (0.45)	1964(2.18)	402 (0.47)
	BC,CD,DE,EF,FG	1964 (2.18)	402 (0.47)	402 (0.45)	402 (0.45)	1964 (2.18)	402 (0.47)
EB5	AB	226 (0.32)	760 (1.07)	226 (0.32)	760 (1.07)	1964 (2.75)	760 (1.07)
	BC,CD,DE,EF	1964 (2.75)	760 (1.07)	226 (0.32)	760 (1.07)	1964 (2.75)	760 (1.07)
EB5	FG,GH,HI,IJ	1964 (2.25)	760 (0.87)	226 (0.26)	760 (0.87)	1964 (2.25)	760 (0.87)
	JK	1964 (2.25)	760 (0.87)	226 (0.26)	760 (0.87)	226 (0.26)	760 (0.87)

lengths 0.25L_i, 0.50L_i and 0.25L_i respectively, are assumed for reinforcement in each span. The reinforcement detailing data for each segment is also given in Table 6(b). Example beams have been chosen in such a way that none of the combinations of input parameters has been used in the training, validating and testing.

The input parameters for the example beams are shown in Table 7. Inelastic mid-span deflections obtained from the proposed closed form expressions (D_{CFE}^{in}), FEM (D_{FEM}^{in}), ACI 318 (2008) expression (D_{ACI}^{in}) and Bischoff (2005) expression (D_{BIS}^{in}) are reported in Table 8. For comparison, the elastic deflections, D^{el} neglecting cracking are also reported.

For FEM results, modeling has been done in the ABAQUS (2011) software (Patel *et al.* 2014, 2015, 2016a, b, c, d, Ramnavas *et al.* 2015, 2017). The beam is modeled using B21 elements (2-node linear Timoshenko beam element in plane). Under service load, the stress-strain

Table 7 Input parameters for the example beams

Beam	Span (i)	Input Parameters											
		C^i	C_i	C^{i+1}	R_{i-1}	R^i	R_i	R^{i+1}	R_{i+1}	S_{i-1}/S_i	S_i/S_{i+1}	w_{i-1}/w_i	w_i/w_{i+1}
EB1	1	-	0.16450.1950	-	-	0.75490.57861.4041	-	1.30	-	2.29	-	-	-
	2	0.19500.1645	-	0.75490.57861.4041	-	-	-	1.30	-	2.29	-	-	
EB2	1	-	0.27800.3870	-	-	1.48320.77361.4549	-	0.73	-	0.37	-	-	
	2	0.38700.27800.3870	1.48320.77361.45490.95644.3505	0.73	0.43	0.37	0.44	-	-	-	-	-	
EB2	3	0.38700.2780	-	1.45490.95644.3505	-	-	0.43	-	0.44	-	-	-	
	1	-	0.12400.1199	-	-	0.65430.61735.9921	-	0.83	-	1.21	-	-	
EB3	2	0.11990.12400.1199	0.65430.61735.9921	1.84332.1260	0.83	0.84	1.21	0.72	-	-	-	-	
	3	0.11990.12400.1199	5.9921	1.84332.12600.94331.3968	0.84	1.06	0.72	1.18	-	-	-	-	
EB3	4	0.11990.1240	-	2.12600.94331.3968	-	-	1.06	-	1.18	-	-	-	
	1	-	0.20900.7160	-	-	1.06520.45610.5683	-	1.13	-	0.63	-	-	
EB4	2	0.71600.20900.7160	1.06520.45610.56830.41400.8575	1.13	0.78	0.63	0.68	-	-	-	-	-	
	3	0.71600.20900.7160	0.56830.41400.85750.42550.5898	0.78	1.29	0.68	1.52	-	-	-	-	-	
EB4	4	0.71600.20900.7160	0.85750.42550.58980.46921.2133	1.29	0.73	1.52	0.69	-	-	-	-	-	
	5	0.71600.20900.7160	0.58980.46921.21330.46600.5838	0.73	1.36	0.69	1.45	-	-	-	-	-	
EB4	6	0.71600.20900.7160	1.21330.46600.58380.43301.0624	1.36	0.56	1.45	0.58	-	-	-	-	-	
	7	0.71600.2090	-	0.58380.43301.0624	-	-	0.56	-	0.58	-	-	-	
EB5	1	-	0.47400.9330	-	-	1.54230.47280.4876	-	1.58	-	1.01	-	-	
	2	0.93300.47400.9330	1.54230.47280.48760.40630.7231	1.58	0.78	1.01	0.66	-	-	-	-	-	
EB5	3	0.93300.47400.9330	0.48760.40630.72310.40650.4899	0.78	1.29	0.66	1.47	-	-	-	-	-	
	4	0.93300.47400.9330	0.72310.40650.48990.42130.7644	1.29	0.89	1.47	0.95	-	-	-	-	-	
EB5	5	0.93300.47400.9330	0.48990.42130.76440.45770.8219	0.89	1.18	0.95	1.25	-	-	-	-	-	
	6	0.93300.41600.83400.76440.45770.82190.59520.9091	1.18	0.80	1.25	0.58	-	-	-	-	-	-	
EB5	7	0.83400.41600.8340	0.82190.59520.90910.45500.5380	0.80	1.27	0.58	1.23	-	-	-	-	-	
	8	0.83400.41600.8340	0.90910.45500.53800.44680.8608	1.27	0.79	1.23	0.71	-	-	-	-	-	
EB5	9	0.83400.41600.8340	0.53800.44680.86080.42640.4971	0.79	1.20	0.71	1.72	-	-	-	-	-	
	10	0.83400.4160	-	0.86080.42640.4971	-	-	1.20	-	1.72	-	-	-	

relationship of concrete is assumed to be linear in compression. Concrete is considered as an elastic material in tension before cracking and softening behavior is assumed linearly after cracking. Tension stiffening is defined in the model using post-failure stress-strain data. In order to define the smeared crack model, the absolute value of the ratio of uniaxial tensile stress at failure to the uniaxial compressive stress at failure is obtained using concrete properties. The plastic strain is taken in accordance with tensile strength of concrete. Further, at service load, the stress in reinforcement is assumed to be in the linear range.

In absence of experimental data, the results from FEM are taken as standard with which the results obtained from the closed form expressions, ACI 318 (2008) expression and Bischoff (2005) expression are compared. The difference between the results from the any of these expressions and FEM is taken as error. It may be noted that small deflections (high L_t/D_t^{el} ratios) are not of any practical significance. Neglecting cases with very high L_t/D_t^{el} ratios (greater than 5000), the maximum absolute percentage errors in D_{CFE}^{in} , D_{ACI}^{in} and D_{BIS}^{in} with respect

Table 8 Comparison of inelastic deflections in the example beams

Beam	Span (i)	Error (%) in								
		D^{el}	D_{CFE}^{in}	D_{FEM}^{in}	D_{ACI}^{in}	D_{BIS}^{in}	(with respect to D_{FEM}^{in})			L_1/D_t^{el}
		(mm)					D_{CFE}^{in}	D_{ACI}^{in}	D_{BIS}^{in}	
EB1	1	4.83	9.46	9.08	9.74	15.13	-4.19	-7.27	-66.63	1677
	2	3.71	4.00	4.24	3.67	3.41	5.66	13.44	19.58	2830
EB2	1	3.96	4.24	4.45	4.30	4.32	4.72	3.37	2.92	2778
	2	1.72	2.01	1.93	1.90	1.89	-4.15	1.55	2.07	4651
	3	0.08	0.04	0.05	0.09	0.08	20.00	-80.00	-60.00	42500
EB3	1	3.90	10.10	9.89	9.75	14.20	-2.12	1.42	-43.58	1795
	2	-0.15	-0.17	-0.24	-0.44	-0.54	29.17	-83.33	-125.00	-38667
	3	0.41	0.40	0.53	0.49	0.52	24.53	7.55	1.89	11951
	4	0.95	1.21	1.07	0.96	0.99	-13.08	10.28	7.48	5474
EB4	1	3.60	4.50	4.29	3.54	3.44	-4.90	17.48	19.81	2222
	2	8.13	18.31	18.89	18.88	20.47	3.07	0.05	-8.36	1107
	3	2.38	1.74	1.77	3.87	4.82	1.69	-118.64	-172.32	2941
	4	7.81	15.53	16.14	17.85	19.52	3.78	-10.59	-20.94	1152
	5	1.08	-0.95	-0.82	0.70	0.60	-15.85	185.37	173.17	6111
	6	7.95	17.22	17.4	17.85	19.33	1.03	-2.59	-11.09	1132
	7	1.38	1.80	1.74	1.46	1.44	-3.45	16.09	17.24	3623
EB5	1	0.88	0.41	0.51	0.69	0.70	19.61	-35.29	-37.25	6477
	2	8.81	15.71	15.23	16.64	15.93	-3.15	-9.26	-4.60	1022
	3	2.61	2.67	2.56	4.65	4.47	-4.30	-81.64	-74.61	2682
	4	8.47	12.58	12.13	16.73	16.02	-3.71	-37.92	-32.07	1063
	5	3.44	3.51	3.89	5.74	5.49	9.77	-47.56	-41.13	2326
	6	4.49	5.38	5.41	7.96	7.78	0.55	-47.13	-43.81	2094
	7	2.01	2.20	2.29	2.82	2.67	3.93	-23.14	-16.59	3731
	8	7.22	11.65	12.47	14.59	14.14	6.58	-17.00	-13.39	1316
	9	1.90	1.30	1.22	2.69	2.64	-6.56	-120.49	-116.39	3947
	10	8.77	18.34	19.88	20.11	19.68	7.75	-1.16	1.01	1026

to D_{FEM}^{in} are 9.77%, 120.49% and 172.32% for all the spans of the beams EB1-EB5 respectively. The root mean square percentage errors in D_{CFE}^{in} , D_{ACI}^{in} and D_{BIS}^{in} with respect to D_{FEM}^{in} are 4.78%, 46.38% and 56.67% for all the spans of the beams EB1-EB5 respectively. Significant errors are observed in D_{ACI}^{in} and D_{BIS}^{in} , whereas, the errors in D_{CFE}^{in} are found to be small and acceptable for practical design. Greater errors in D_{ACI}^{in} and D_{BIS}^{in} may be due to adoption of ACI 435 (2000) procedure which considered simplified assumptions for evaluation of a weighted average effective moment of inertia in continuous beams. This shows the efficacy of the developed methodology for continuous beams with any number of spans.

The procedures available in literature or any other commercial software based on finite element analysis that incorporate concrete cracking would require reinforcement detailing data. It would be tedious to provide such reinforcement detailing data for every element in a large

structure since reinforcement lengths and cross-section areas may vary from element to element. Further, details like post-cracking stress-strain relationship would also be required. It is not feasible to carry out such elaborate computations for the day to day design particularly preliminary design. The convergence problem may also be encountered in FEA. On the other hand, the present methodology requires only cross-sectional properties, elastic moments, elastic deflections and reinforcement data at three locations.

When the closed form expressions are used, the computational time is drastically reduced and it is a fraction of that required for Type 1 and Type 2 procedures available in literature. It was observed by Patel *et al.* (2014) that in finite element analysis, usually 16-32 elements in a span are required for convergence of results within 1% and the computational effort required in the analytical-numerical procedure is about 1-3% of that required in FEA. It may be noted that the analytical-numerical procedure (Patel *et al.* 2014) typically requires five iterations for convergence whereas ANN technique requires only one analysis. The computational effort required in the proposed technique of use of closed form expressions can therefore be estimated to be about 0.2-0.6% of FEA. This reduction in computational effort is quite significant for structures with a large number of degrees of freedom.

8. Conclusions

A methodology, using neural networks, has been presented for rapid prediction of deflections in reinforced concrete beams subjected to service load. Closed form expressions, obtained from the trained neural networks, have been proposed for predicting the inelastic deflections taking into account concrete cracking and tension stiffening effect. Five separate neural networks are developed for prediction of inelastic deflections from the elastic moments and deflections having any number of spans. Data sets for neural networks are generated using the computationally efficient analytical-numerical procedure recently developed by authors. The proposed expressions have been verified for a number of example beams. The proposed expressions require minimal input data and computation effort and yield results that are close to FEM results and experimental results. The root mean square percentage error in deflections obtained from the proposed closed form expression is 6.74% with respect to the experimental results for simply supported beams reported in literature. For continuous beams, the root mean square percentage error in deflections obtained from the proposed closed form expressions is 4.78% with respect to FEM results. These errors are small for practical purposes, therefore the proposed expressions can be used in every day design.

The methodology can be extended for large RC building frames for use in every day design. The methodology can also be extended to account for shear deformation in beams with low span-effective depth ratios (Wang *et al.* 2015).

References

- ABAQUS (2011), *ABAQUS Standard User's Manuals*, Karlsson and Sorensen Inc., Rhode Island, U.S.A.
- ACI 318 (2008), *Building Code Requirements for Structural Concrete and Commentary*, U.S.A.
- ACI 435 (2000), *Control of Deflection in Concrete Structures*, U.S.A.
- Bathe, K.J. (2002), *Finite Element Procedures*, 6th Edition, Prentice-Hall Pvt. Ltd., New Delhi, India.
- Bischoff, P.H. (2005), "Reevaluation of deflection prediction for concrete beams reinforced with steel and fiber reinforced polymer bars", *J. Struct. Eng.*, **131**(5), 752-767.
- Caglar, N., Pala, M., Elmas, M. and Eryilmaz, D.M. (2009), "A new approach to determine the base shear of steel frame structures", *J. Constr. Steel Res.*, **65**(1), 188-195.
- Casanova, A., Jason, L. and Davenne, L. (2012), "Bond slip model for the simulation of reinforced concrete structures", *Eng. Struct.*, **39**, 66-78.
- Chan, C.M., Mickleborough, N.C. and Ning, F. (2000), "Analysis of cracking effects on tall reinforced concrete buildings", *J. Struct. Eng.*, **126**(9), 995-1003.
- Chan, C.M., Ning, F. and Mickleborough, N.C. (2000), "Lateral stiffness characteristics of tall reinforced concrete buildings under service loads", *Struct. Des. Tall Build.*, **9**(5), 365-383.
- Chaudhary, S., Pendharkar, U. and Nagpal, A.K. (2007), "Bending moment prediction for continuous composite beams by neural networks", *Adv. Struct. Eng.*, **10**(4), 439-454.
- Chaudhary, S., Pendharkar, U., Patel, K.A. and Nagpal, A.K. (2014), "Neural networks for deflections in continuous composite beams considering concrete cracking", *Iran. J. Sci. Technol. Trans. Civil Eng.*, **38**(C1⁺), 205-221.
- CSA A23.3 (2004), *Design of Concrete Structures*, Canada.
- Dai, J.G., Ueda, T., Sato, Y. and Nagai, K. (2012), "Modeling of tension stiffening behavior in FRP-strengthened RC members based on rigid body spring networks", *Comput. Aid. Civil Infrastruct. Eng.*, **27**(6), 406-418.
- Dias, J.L.R. and Silvestre, N. (2011), "A neural network based closed-form solution for the distortional buckling of elliptical tubes", *Eng. Struct.*, **33**(6), 2015-2024.
- Dundar, C. and Kara, I.F. (2007), "Three dimensional analysis of reinforced concrete frames with cracked beam and column elements", *Eng. Struct.*, **29**(9), 2262-2273.
- Gedam, B.A., Bhandari, N.M. and Upadhyay, A. (2014), "An apt material model for drying shrinkage and specific creep of HPC using artificial neural network", *Struct. Eng. Mech.*, **52**(1), 97-113.
- Gupta, R.K., Kumar, S., Patel, K.A., Chaudhary, S. and Nagpal, A.K. (2015), "Rapid prediction of deflections in multi-span continuous composite bridges using neural networks", *J. Steel Struct.*, **15**(4), 893-909.
- Gupta, R.K., Patel, K.A., Chaudhary, S. and Nagpal, A.K. (2013), "Closed form solution for deflection of flexible composite bridges", *Proc. Eng.*, **51**, 75-83.
- Joshi, S.G., Londhe, S.N. and Kwatra, N. (2014), "Application of artificial neural networks for dynamic analysis of building frames", *Comput. Concrete*, **13**(6), 765-780.
- Kalkan, İ. (2010), "Deflection prediction for reinforced concrete beams through different effective moment of inertia expressions", *J. Eng. Res. Dev.*, **2**(1), 72-80.
- Kara, I.F. and Dundar, C. (2009), "Effect of loading types and reinforcement ratio on an effective moment of inertia and deflection of a reinforced concrete beam", *Adv. Eng. Soft.*, **40**(9), 836-846.
- Kara, I.F. and Dundar, C. (2010), "Three-dimensional analysis of tall reinforced concrete buildings with nonlinear cracking effects", *Mech. Based Des. Struct. Mach.*, **38**(3), 388-402.
- Khan, M.I. (2012), "Predicting properties of high performance concrete containing composite cementitious materials using artificial neural networks", *Automat. Constr.*, **22**, 516-524.
- Kim, D.K., Kim, D.H., Cui, J., Seo, H.Y. and Lee, Y.H. (2009), "Iterative neural network strategy for static model identification of an FRP deck", *Steel Compos. Struct.*, **9**(5), 445-455.
- MATLAB 7.8 (2009), *Neural Networks Toolbox User's Guide*, U.S.A.
- Mohammadhassani, M., Nezamabadi-Pour, H., Jumaat, M.Z., Jameel, M. and Arumugam, A.M.S. (2013a), "Application of artificial neural networks (ANNs) and linear regressions (LR) to predict the deflection of concrete deep beams", *Comput. Concrete*, **11**(3), 237-252.
- Mohammadhassani, M., Nezamabadi-Pour, H., Jumaat, M.Z., Jameel, M., Hakim, S.J.S. and Zargar, M. (2013b), "Application of the ANFIS model in deflection prediction of concrete deep beam", *Struct. Eng. Mech.*, **45**(3), 319-332.
- Mohr, S., Bairán, J.M. and Mari, A.R. (2010), "A frame element model for the analysis of reinforced concrete structures under shear and bending", *Eng. Struct.*, **32**(12), 3936-3954.
- Pala, M. (2006), "A new formulation for distortional buckling stress in cold-formed steel members", *J. Constr. Steel Res.*, **62**(7), 716-722.
- Patel, K.A., Bhardwaj, A., Chaudhary, S. and Nagpal, A.K. (2015), "Explicit expression for effective moment of inertia of RC Beams", *Lat. Am. J. Solid Struct.*, **12**(3), 542-560.
- Patel, K.A., Chaudhary, S. and Nagpal, A.K. (2014), "Analytical-numerical procedure incorporating cracking in RC beams", *Eng. Comput.*, **31**(5), 986-1010.
- Patel, K.A., Chaudhary, S. and Nagpal, A.K. (2016a), "A tension stiffening model for analysis of RC flexural members under service load", *Comput. Concrete*, **17**(1), 29-51.
- Patel, K.A., Chaudhary, S. and Nagpal, A.K. (2016b), "An element incorporating cracking for reinforced concrete skeletal structures at service load", *Adv. Struct. Eng.*, 1369433216673642.
- Patel, K.A., Chaudhary, S. and Nagpal, A.K. (2016c), "Rapid prediction of inelastic bending moments in RC beams considering cracking", *Comput. Concrete*, **18**(3), 1113-1134.
- Patel, K.A., Chaudhary, S. and Nagpal, A.K. (2016d), "An automated computationally efficient two stage procedure for service load analysis of RC flexural members considering concrete cracking", *Eng. Comput.*, 1-20
- Pendharkar, U., Chaudhary, S. and Nagpal, A.K. (2007), "Neural network for bending moment in continuous composite beams considering cracking and time effects in concrete", *Eng. Struct.*, **29**(9), 2069-2079.
- Pendharkar, U., Chaudhary, S. and Nagpal, A.K. (2010), "Neural networks for inelastic mid-span deflections in continuous composite beams", *Struct. Eng. Mech.*, **36**(2), 165-179.
- Pendharkar, U., Chaudhary, S. and Nagpal, A.K. (2011), "Prediction of moments in composite frames considering cracking and time effects using neural network models", *Struct. Eng. Mech.*, **39**(2), 267-285.
- Pendharkar, U., Patel, K.A., Chaudhary, S. and Nagpal, A.K. (2015), "Rapid prediction of long-term deflections in composite frames", *Steel Compos. Struct.*, **18**(3), 547-563.
- Pendharkar, U., Patel, K.A., Chaudhary, S. and Nagpal, A.K. (2016a), "Rapid prediction of moments in high-rise composite frames considering cracking and time-effects", *Period. Polytech. Civil Eng.*
- Pendharkar, U., Patel, K.A., Chaudhary, S. and Nagpal, A.K. (2016b), "Closed form expressions for long-term deflections in high-rise composite frames", *J. Steel Struct.*, **17**(1).
- Ramnavas, M.P., Patel, K.A., Chaudhary, S. and Nagpal, A.K. (2015), "Cracked span length beam element for service load analysis of steel concrete composite bridges", *Comput. Struct.*, **157**, 201-208.
- Ramnavas, M.P., Patel, K.A., Chaudhary, S. and Nagpal, A.K.

- (2017), "Service load analysis of composite frames using cracked span length frame element", *Eng. Struct.*, **132**, 733-744.
- Saechai, S., Kongprawechnon, W. and Sahamitmongkol, R. (2012), "Test system for defect detection in construction materials with ultrasonic waves by support vector machine and neural network", *Proceedings of the International SCIS-ISIS Conference*, November.
- Saechai, S., Kusalangoorawat, P., Kongprawechnon, W. and Sahamitmongkol, R. (2011), "New developed testing system of defect in cementitious material with neural network", *Proceedings of the 8th International ECTI Conference*, May.
- Scanlon, A., Cagley O.D.R. and Buettner, D.R. (2001), "ACI code requirements for deflection control: A critical review", *ACI SP* **203**, 1-14.
- Shahin, M. and Elchanakani, M. (2008), "Neural networks for ultimate pure bending of steel circular tubes", *J. Constr. Steel Res.*, **64**(6), 624-633.
- Stramandinoli, R.S.B. and Rovere, H.L.L. (2008), "An efficient tension-stiffening model for nonlinear analysis of reinforced concrete members", *Eng. Struct.*, **30**(7), 2069-2080.
- Stramandinoli, R.S.B. and Rovere, H.L.L. (2012), "FE model for nonlinear analysis of reinforced concrete beams considering shear deformation", *Eng. Struct.*, **35**, 244-253.
- Tadesse, Z., Patel, K.A., Chaudhary, S. and Nagpal, A.K. (2012), "Neural networks for prediction of deflection in composite bridges", *J. Constr. Steel Res.*, **68**(1), 138-149.
- Tanrikulu, A.K., Dundar, C. and Cagatay, I.H. (2000), "A computer program for the analysis of reinforced concrete frames with cracked beam elements", *Struct. Eng. Mech.*, **10**(5), 463-478.
- Tohidi, S. and Sharifi, Y. (2015), "Neural networks for inelastic distortional buckling capacity assessment of steel I-beams", *Thin Wall Struct.*, **94**, 359-371.
- Wang, T. and Hsu, T.T.C. (2001), "Nonlinear finite element analysis of concrete structures using new constitutive models", *Comput. Struct.*, **79**(32), 2781-2791.
- Wang, T., Dai, J.G. and Zheng, J.J. (2015), "Multi-angle truss model for predicting the shear deformation of RC beams with low span-effective depth ratios", *Eng. Struct.*, **91**, 85-95.
- Yang, Z.J. and Chen, J. (2005), "Finite element modelling of multiple cohesive discrete crack propagation in reinforced concrete beams", *Eng. Fract. Mech.*, **72**(14), 2280-2297.

CC

Notations

- A_{st}, A_{sb} area of top and bottom reinforcement respectively
- B, D width and total depth of section respectively
- C, R inertia ratio and cracking moment respectively
- D^{el}, D^{in} elastic and inelastic deflection respectively
- D^{ss} elastic deflection of an equivalent simply supported beam
- E modulus of elasticity
- I moment of inertia about neutral axis
- I_j j^{th} input parameter
- L, O length of the span and stiffness respectively
- M^{el}, M^{in} elastic and inelastic moment respectively
- O output parameter
- $bias$ bias of hidden or output neuron

- d_t, d_b effective concrete cover at top and bottom respectively
- f_t, f_c' tensile strength and cylinder compressive strength respectively
- h_k k^{th} hidden neuron
- q number of input parameters
- r number of hidden neurons
- w, x uniformly distributed load and cracked length respectively
- $W_{j,k}^{jh}$ weight of the link between I_j and h_c
- $W_{k,1}^{ho}$ weight of the link between h_c and O
- ρ_{st}, ρ_{sb} percentage steel reinforcement at top and bottom respectively

Subscript

- A, B ends A and B of a cracked span length beam element respectively
- S in-span position of a cracked span length beam element
- c, s concrete and steel respectively
- f, w flange and web respectively
- i i^{th} span
- j, o input and output neuron number respectively
- k hidden neuron number or function number

Superscript

- cr, un cracked and uncracked respectively
- el, in elastic and inelastic respectively
- g gross
- ho connection between hidden and output layers
- i i^{th} support
- ih connection between input and hidden layers

Appendix A

Closed form expressions for value of O

(I) External span of two span continuous beams

(a) Left external span

$$O = \frac{4.00}{1+e^{-\left(\frac{10.10}{1+e^{-H_1}} + \frac{22.38}{1+e^{-H_2}} + \frac{12.64}{1+e^{-H_3}} + \frac{9.49}{1+e^{-H_4}} + \frac{3.13}{1+e^{-H_5}} + \frac{19.90}{1+e^{-H_6}} + \frac{28.70}{1+e^{-H_7}} + \frac{10.13}{1+e^{-H_8}} + \frac{25.77}{1+e^{-H_9}} + \frac{24.76}{1+e^{-H_{10}}}\right)}} - 1.00 \quad (A1)$$

$$\begin{bmatrix} H_1 \\ H_2 \\ H_3 \\ H_4 \\ H_5 \\ H_6 \\ H_7 \\ H_8 \\ H_9 \\ H_{10} \end{bmatrix} = \begin{bmatrix} 3.80 & 1.47 & 12.27 & -3.22 & -0.24 & 3.49 & -0.87 \\ -2.81 & -1.75 & -12.58 & 4.12 & 0.23 & -3.53 & 0.68 \\ -4.89 & -1.31 & -12.37 & 2.50 & 0.28 & -3.95 & 1.17 \\ 0.76 & 3.59 & -0.34 & 13.60 & -0.40 & -0.45 & 0.35 \\ -0.38 & -1.05 & -1.22 & 4.52 & -22.83 & -9.07 & 6.85 \\ 0.70 & 1.15 & -0.41 & -5.51 & 23.52 & 9.41 & -6.12 \\ 27.47 & -0.11 & 0.45 & 12.37 & 0.64 & 2.33 & -1.34 \\ -24.54 & -0.94 & -7.48 & -3.30 & -0.44 & -2.09 & 1.21 \\ 14.92 & 10.83 & 2.14 & 11.23 & -0.27 & -1.10 & 0.34 \\ -10.80 & 1.79 & 0.61 & -1.78 & 0.12 & 11.58 & -7.51 \end{bmatrix} + \begin{bmatrix} C_1 \\ C_2 \\ R_1 \\ R_2 \\ S_1/S_2 \\ w_1/w_2 \end{bmatrix} = \begin{bmatrix} -3.80 \\ 3.25 \\ 4.59 \\ 0.29 \\ -0.98 \\ 0.37 \\ -1.29 \\ 0.91 \\ 0.08 \\ -3.92 \end{bmatrix} \quad (A2)$$

(b) Right external span

The value of O for right external span can be obtained by replacing $C_1, R_1, R_2, S_1/S_2$ and w_1/w_2 in Eq. (A2) with $C_2, R_2, R_1, S_2/S_1$ and w_2/w_1 respectively.

(II) External span of multi span continuous beams

(a) Left external span

$$O = \frac{4.40}{1+e^{-\left(\frac{4.95}{1+e^{-H_1}} + \frac{19.22}{1+e^{-H_2}} + \frac{6.18}{1+e^{-H_3}} + \frac{7.11}{1+e^{-H_4}} + \frac{9.64}{1+e^{-H_5}} + \frac{0.37}{1+e^{-H_6}} + \frac{0.06}{1+e^{-H_7}} + \frac{9.76}{1+e^{-H_8}} + \frac{5.56}{1+e^{-H_9}} + \frac{0.19}{1+e^{-H_{10}}}\right)}} - 0.70 \quad (A3)$$

$$\begin{bmatrix} H_1 \\ H_2 \\ H_3 \\ H_4 \\ H_5 \\ H_6 \\ H_7 \\ H_8 \\ H_9 \\ H_{10} \end{bmatrix} = \begin{bmatrix} -31.81 & -13.27 & -1.23 & -18.65 & -0.04 & -1.74 & 1.09 \\ 4.16 & 2.34 & 21.54 & -3.49 & -0.62 & 0.59 & -0.04 \\ -4.83 & -1.79 & -17.72 & 2.81 & 0.48 & 0.04 & -0.03 \\ -1.28 & -3.26 & -0.07 & -8.54 & 0.86 & 0.45 & -0.50 \\ 6.52 & 1.95 & 0.44 & 2.90 & 1.29 & -4.89 & 3.18 \\ -1.48 & -1.63 & -5.05 & -1.55 & 0.30 & 3.92 & 17.16 \\ 12.15 & -0.25 & -0.96 & -1.35 & 10.92 & -0.73 & 0.20 \\ 0.23 & 3.62 & 4.75 & -5.43 & -1.61 & 0.42 & 0.40 \\ -5.33 & 2.59 & -4.16 & -2.78 & 5.04 & -1.18 & -3.55 \\ 18.70 & 1.95 & 17.26 & -5.99 & 0.14 & -1.63 & -0.21 \end{bmatrix} + \begin{bmatrix} C_1 \\ C_2 \\ R_1 \\ R_2 \\ S_1/S_2 \\ w_1/w_2 \end{bmatrix} = \begin{bmatrix} 2.07 \\ -3.62 \\ 3.24 \\ -1.03 \\ -3.59 \\ -1.53 \\ 1.00 \\ 2.22 \\ 2.15 \\ 0.36 \end{bmatrix} \quad (A4)$$

(b) Right external span

The value of O for right external span can be obtained by replacing $C_1, R_1, R_2, S_1/S_2$ and w_1/w_2 in Eq. (A4) with $C_n, R_n, R_{n-1}, S_n/S_{n-1}$ and w_n/w_{n-1} respectively, where n denotes the number of spans in the beam.

(III) Penultimate span of multi span continuous beams

$$O = \frac{4.00}{1+e^{-\left(\frac{25.58}{1+e^{-H_1}} + \frac{0.01}{1+e^{-H_2}} + \frac{0.01}{1+e^{-H_3}} + \frac{1.64}{1+e^{-H_4}} + \frac{0.02}{1+e^{-H_5}} + \frac{0.01}{1+e^{-H_6}} + \frac{7.63}{1+e^{-H_7}} + \frac{0.03}{1+e^{-H_8}}\right)}} \quad (A5)$$

$$\frac{4.20}{1+e^{-\left(\frac{0.01}{1+e^{-H_8}} + \frac{0.31}{1+e^{-H_9}} + \frac{4.69}{1+e^{-H_{10}}} + \frac{17.61}{1+e^{-H_{11}}} + \frac{3.31}{1+e^{-H_{12}}} + \frac{0.07}{1+e^{-H_{13}}} + \frac{4.68}{1+e^{-H_{14}}} + \frac{0.03}{1+e^{-H_{15}}} + \frac{0.96}{1+e^{-H_{16}}}\right)}} - 1.40$$

$$\begin{bmatrix} H_1 \\ H_2 \\ H_3 \\ H_4 \\ H_5 \\ H_6 \\ H_7 \\ H_8 \\ H_9 \\ H_{10} \\ H_{11} \\ H_{12} \\ H_{13} \\ H_{14} \\ H_{15} \\ H_{16} \end{bmatrix} = \begin{bmatrix} -1.57 & -2.01 & 0.00 & -6.38 & 8.92 & -3.78 & -9.93 & 5.29 & -32.49 & 28.69 & 9.05 & -24.31 \\ 0.71 & -5.74 & -7.82 & -0.83 & 8.51 & 3.94 & 0.62 & -0.09 & -1.21 & -6.50 & -3.27 & 10.70 \\ -0.75 & -5.98 & -0.19 & 0.98 & 1.28 & -10.16 & -2.07 & -0.67 & -1.02 & -4.66 & -0.05 & 2.09 \\ 20.76 & -1.85 & 15.06 & 7.80 & -18.94 & 18.34 & 3.72 & 6.91 & 4.27 & -10.30 & 3.67 & 5.14 \\ -35.84 & 7.15 & -0.62 & -23.06 & 43.97 & 3.64 & 21.74 & -35.61 & 7.41 & 29.29 & 3.70 & 2.90 \\ -7.86 & -11.40 & -3.75 & 1.03 & -15.18 & -5.80 & 6.04 & 0.06 & -1.51 & 0.73 & 0.52 & 0.17 \\ -2.50 & -14.76 & 1.93 & 3.50 & 11.96 & -6.06 & -5.75 & 1.57 & 11.52 & 6.56 & -1.42 & -3.59 \\ 13.11 & 4.23 & 4.81 & -21.39 & -19.50 & -28.56 & 18.57 & -0.42 & -29.02 & 21.10 & -9.45 & 3.15 \\ 1.23 & 5.84 & 1.10 & 1.17 & -1.24 & -0.28 & -0.96 & 0.42 & -1.23 & -5.29 & 0.74 & 2.27 \\ -0.44 & 10.15 & -0.80 & -0.13 & 0.41 & -1.37 & -0.27 & 9.45 & 1.98 & -1.41 & -0.58 & 1.04 \\ 1.33 & 2.92 & -0.28 & -1.01 & -1.42 & -0.24 & 7.43 & 1.65 & 1.17 & 13.78 & -0.41 & -5.57 \\ 0.13 & 3.07 & 0.63 & 18.22 & -2.94 & -0.02 & -1.26 & 0.15 & 4.34 & 0.26 & -0.62 & -0.55 \\ 2.14 & 0.73 & -0.96 & -0.02 & -2.09 & -0.24 & 17.86 & -0.41 & -6.00 & 19.30 & 1.92 & -8.57 \\ -0.55 & -1.94 & -5.61 & 0.12 & 0.43 & 0.35 & -10.87 & -0.42 & -0.43 & -0.75 & -0.06 & 0.24 \\ 1.11 & -10.13 & 0.37 & 0.75 & -18.34 & -0.01 & 10.96 & 1.90 & 3.08 & -9.11 & -1.44 & 2.76 \\ 5.69 & 1.80 & -0.15 & -0.04 & 13.44 & -1.12 & 0.83 & 0.49 & 1.89 & 3.35 & -0.94 & -1.62 \end{bmatrix} + \begin{bmatrix} C \\ C_1 \\ C_2 \\ R_{-1} \\ R \\ R_1 \\ R_2 \\ S_{-1}/S_1 \\ S_1/S_2 \\ w_{-1}/w_1 \\ w_1/w_{-1} \end{bmatrix} = \begin{bmatrix} 15.26 \\ 1.06 \\ 2.20 \\ -33.75 \\ 17.20 \\ 0.50 \\ -3.11 \\ 22.28 \\ -0.37 \\ 2.22 \\ 1.39 \\ 0.38 \\ -3.28 \\ -0.49 \\ 0.95 \\ -1.29 \end{bmatrix} \quad (A6)$$

(IV) Internal span of multi span continuous beams

$$O = \frac{4.00}{1+e^{-\left(\frac{6.31}{1+e^{-H_1}} + \frac{0.01}{1+e^{-H_2}} + \frac{11.65}{1+e^{-H_3}} + \frac{1.28}{1+e^{-H_4}} + \frac{5.06}{1+e^{-H_5}} + \frac{11.65}{1+e^{-H_6}} + \frac{3.49}{1+e^{-H_7}} + \frac{4.89}{1+e^{-H_8}}\right)}} - 0.95 \quad (A7)$$

$$\begin{bmatrix} H_1 \\ H_2 \\ H_3 \\ H_4 \\ H_5 \\ H_6 \\ H_7 \\ H_8 \\ H_9 \\ H_{10} \\ H_{11} \\ H_{12} \\ H_{13} \\ H_{14} \\ H_{15} \\ H_{16} \end{bmatrix} = \begin{bmatrix} -3.87 & 0.77 & 4.24 & -0.48 & 0.93 & 2.23 & 1.57 & -2.28 & 8.74 & 2.71 & 3.53 & 0.65 \\ 0.38 & -11.58 & 0.91 & -0.20 & -0.28 & 1.86 & -0.47 & -5.41 & -1.16 & 1.11 & 0.28 & -0.91 \\ 0.16 & 1.36 & -3.73 & -0.21 & 0.31 & -0.43 & 4.41 & -0.15 & -0.89 & 6.34 & 0.32 & -2.83 \\ 0.75 & -6.64 & -0.54 & -12.19 & 0.89 & 0.13 & 1.04 & -0.25 & 1.38 & -0.97 & -0.92 & 0.66 \\ 1.63 & 0.40 & 0.11 & 0.63 & 2.07 & -0.21 & -0.04 & 0.26 & -1.44 & 1.40 & 0.43 & -0.68 \\ -3.06 & -0.89 & -0.15 & -0.93 & -2.96 & 0.37 & -0.06 & -0.35 & 2.42 & -2.33 & -0.74 & 1.17 \\ -0.05 & 2.08 & 8.11 & -0.45 & 0.39 & -0.01 & 9.17 & -0.08 & 2.43 & -1.37 & -0.46 & 0.86 \\ 6.45 & 0.72 & 2.53 & -2.65 & -2.79 & -3.04 & -0.95 & -3.51 & 5.96 & -3.89 & -2.09 & -6.56 \\ -2.09 & 3.15 & 0.14 & 0.79 & 1.26 & 0.49 & -0.47 & 0.68 & 0.78 & 1.46 & 0.00 & -0.58 \\ -1.49 & 1.34 & 0.12 & 0.63 & 0.55 & 0.38 & -0.32 & 0.45 & -0.10 & 1.13 & 0.15 & -0.41 \\ -0.20 & 0.12 & -0.15 & -0.72 & -0.69 & 0.16 & -0.02 & -0.41 & 1.21 & -1.36 & -0.42 & 0.54 \\ 0.18 & -1.29 & -0.07 & 0.50 & -0.78 & -0.38 & -0.05 & 0.25 & -1.31 & 1.27 & 0.39 & -0.46 \\ -0.86 & 0.15 & 0.76 & 2.09 & 3.69 & -0.61 & -0.73 & 0.45 & -6.22 & -1.28 & 5.59 & 0.25 \\ 0.15 & -1.27 & 2.23 & 0.27 & -0.78 & 0.03 & -0.82 & 0.31 & 0.25 & -3.46 & -0.16 & 1.51 \\ 0.48 & 5.46 & 0.64 & -0.89 & 0.69 & 9.68 & -2.40 & -0.27 & 3.02 & -1.06 & -0.78 & 0.10 \\ -11.53 & -19.36 & -7.45 & 0.78 & -5.90 & -6.45 & -0.24 & 0.14 & -3.09 & 0.55 & 1.03 & 0.11 \end{bmatrix} + \begin{bmatrix} C \\ C_1 \\ C_2 \\ R_{-1} \\ R \\ R_1 \\ R_2 \\ S_{-1}/S_1 \\ S_1/S_2 \\ w_{-1}/w_1 \\ w_1/w_{-1} \end{bmatrix} = \begin{bmatrix} -1.76 \\ -3.34 \\ 0.22 \\ -0.85 \\ -2.84 \\ 4.70 \\ 1.06 \\ 2.84 \\ -0.60 \\ -2.16 \\ 1.07 \\ 0.61 \\ -2.99 \\ -0.45 \\ 0.95 \\ 1.32 \end{bmatrix} \quad (A8)$$